

## RESEARCH ARTICLE

# Examination of the influence of printing parameters for the continuous carbon fiber-reinforced thermoplastics based on fused deposition modeling

Altuğ Uşun<sup>\*1</sup>, Recep Gümrük<sup>1</sup>, Nuri Yıldız<sup>1</sup>, Bahri Barış Vatandaş<sup>1</sup><sup>1</sup>Karadeniz Technical University, Department of Mechanical Engineering, Trabzon, Türkiye

## Article Info

### Article history:

Received: 20.11.2021

Revised: 21.07.2022

Accepted: 01.08.2022

Published Online: 16.08.2022

### Keywords:

Continuous fiber-reinforced

thermoplastic (CFRTP)

Fused deposition modelling

Additive manufacturing

Mechanical properties

## Abstract

The continuous carbon fiber-reinforced thermoplastic (CFRTP) printing process has been used more widely in recent years and is an alternative production method, especially in sectors such as aviation, automotive, prototyping, medical applications, and aerospace. Although additive manufacturing reduces the design limitations and makes it easier to manufacture, it is one of the disadvantages of this method: it has relatively low thermal and mechanical properties compared to standard production techniques. Therefore, in this study, printing parameters such as nozzle temperature, printing speed, layer thickness, and heated bed temperatures were investigated for fused deposition modeling. In this regard, a polymer impregnation line based on the melt impregnation technique was utilized to obtain CFRTP filaments using polylactic acid (PLA) and 3K carbon fiber. Obtained filaments were then used to print three-point bending test samples in order to investigate mechanical performance. The test result showed flexural strength between 108 and 224 MPa and flexural modulus between 9.67 and 17.69 GPa with a 23% fiber ratio. Results from this study proclaim that CFRTPs manufactured with this method and optimized printing parameters have great potential for implementing future production methods.

## 1. Introduction

Additive manufacturing (AM) makes the fabrication of the parts with complex geometries using computer-aided design (CAD) data possible, which would have been impossible or very difficult to manufacture using conventional methods. In addition, it does not require molds or expensive tooling. Furthermore, AM can be used to produce components that have been obtained from topology optimizations [1,2] or even cellular structures [3,4] that are implemented inside of the part to decrease the weight while increasing relative strength. Therefore, AM has aroused interest, especially in the aviation and automotive sectors.

AM is a process of obtaining a three-dimensional part using two-dimensional slices called layers. Since the layers have low bonding strength with previous layers, AM printed parts have much lower mechanical properties when compared with conventional manufacturing methods [5,6]. Implementing continuous fiber-reinforced thermoplastic (CFRTP) composites to the printing process has shown great potential to increase the mechanical properties significantly. In addition, CFRTPs have chemical resistance, recyclability, electrical conductivity, and lightness [7,8]. Therefore, it is a serious alternative material group to thermoset composite and metal structures. Various studies were conducted to use the high mechanical properties of CFRTP parts in practical applications [9]. Some of the most prominent examples are given by Markforged. They have produced a certified lifting tool [10] that is 75% lighter than its counterpart. Another example of Markforged is a 7-axis robotic arm which cuts the production time by 70% and production costs by 58% [11].

CFRTP materials can be produced by consolidated automatic fiber laying, thermal forming, continuous compression molding, etc. These methods can be used successfully in producing parts without relatively complex geometries. Therefore, fused deposition modeling (FDM) is used to obtain rather complex CFRTP parts. In the literature, there has been an increasing interest in the production of CFRTPs by additive manufacturing, especially since 2015 [12,13]. In the production of CFRTP, there are two methods, namely, on-nozzle impregnation and the usage of pre-preg filaments. Matsuzaki et al. [14] developed an in-situ production technique that combines continuous carbon fiber and polymer at the nozzle. In this method, thermoplastic material and continuous fiber additives are mixed with the heat in the printer's nozzle before printing. However, the relatively short fiber-polymer mixture zone on the nozzle causes insufficient wetting of the fiber yarns. In the pre-preg filament method, the fiber-polymer filament is obtained by combining thermoplastic and fiber on a different platform. Although this process causes an additional manufacturing process, a much more homogeneous fiber-polymer mixture is obtained compared to the in-nozzle production method, where dry fiber and polymer are mixed during printing.

CFRTP samples printed using pre-preg filament result in very high mechanical properties compared with the thermoplastic resin. For example, Li et al. [15] used PLA with %15 continuous carbon fiber content and achieved average tensile strength of 106.3 MPa. Similarly, Araya-Calvo et al. [16] have achieved 231 MPa flexural strength and 14.17 GPa flexural modulus using the PA6 matrix. Although acquiring

Corresponding Author: Altuğ Uşun  
E-mail: altug@ktu.edu.tr

How to cite this article:

Uşun, A., Gümrük, R., Yıldız N., Vatandaş, B.B., Examination of the influence of printing parameters for the continuous carbon fiber-reinforced thermoplastics based on fused deposition modeling, The International Journal of Materials and Engineering Technology (TIJMET), 2022, 5(2): 65-70

higher mechanical properties, studies were conducted to increase them further. One of the methods to achieve higher mechanical properties is by finding out the ideal printing parameters. Chacon et al. [17] have investigated the mechanical properties of carbon fiber, Kevlar fibers, and glass fibers under different printing parameters. They investigated the build orientation, layer thickness, and fiber ratio. The best results were obtained from flat-oriented parts with 26.38% fiber content, with around 473.3 MPa tensile strength and 525.6 MPa flexural strength using nylon thermoplastic resin. Chen et al. [18] have investigated PLA-glass fiber CFRTP samples. This study investigated the effects of nozzle diameter, nozzle edge width, layer thickness, printing speed, and temperatures. Using the optimal printing parameters, 312 MPa flexural strength and 21.5 GPa flexural modulus were achieved. To further increase the mechanical properties, additional methods were utilized [19], such as the addition of a micro extruder impregnation platform [20] which achieves much higher quality in the mixture of fiber-polymer. Another example would be the addition of a pressure roller that presses the newly printed parts to the printing bed to decrease the voids inside of the printed parts [21]. Some studies in the literature utilized post-processing methods such as heat treatments [22–24] to increase the mechanical properties of CFRTP.

In this study, the printing parameters of CFRTP samples were investigated. Test samples were produced by changing nozzle temperature, heated bed temperature, layer thickness, and printing speed. Pre-preg filament was manufactured using the melt impregnation method to obtain Poly-lactic acid (PLA) and carbon fiber-based CFRTP filaments with high mechanical properties. FDM-based printing was utilized to manufacture CFRTP samples additively. The effects of printing parameters on mechanical properties were investigated. The produced samples were compared using the three-point bending tests.

## 2. Materials and methods

### 2.1. Materials

Poly(lactic acid (PLA) from the eSUN commercial brand, which has 60 MPa tensile and 87 MPa flexural strength, was used for matrix material to obtain CFRTP samples. Carbon fiber (3K) was used as reinforcement. Carbon fibers have 4900 MPa tensile strength, 245 GPa elasticity modulus, and 1.8 g/cm<sup>3</sup> density. CFRTP filaments were manufactured from PLA and carbon fiber using a melt impregnation line from our previous study [25]. This melt impregnation line consists of three main sections: fiber spreading zone, polymer mixture zone, and mold. The fiber spreading zone consists of 5 rollers that spread the fiber laterally by utilizing the normal force along the fiber. This spreading is essential to achieve a homogenous mixture of the fiber-polymer mixture. Next, thermoplastic resin is applied to the fibers in the polymer mixture zone. Finally, in the molding zone, the filament is rounded with heated nozzles to achieve a circular cross-sectional filament to be used in additive manufacturing. Obtained CFRTP filaments have 22% fiber fraction, 446 MPa tensile strength, and 28.40 GPa elasticity modulus.

### 2.2. Manufacturing of CFRTP samples

CFRTP test samples were manufactured using a custom 3D printer that utilizes the FDM technique. Slicing the sample geometries was achieved with a custom G-code to make printing without cutting possible. Printing parameters are summarized in Table 1. The table shows that 210 °C nozzle temperature, 25°C

bed temperature, 0.25 mm layer thickness, and 3000 mm/min were kept constant while other parameters were parametrically investigated.

**Table 1.** Printing parameters for CFRTP samples

Parameter	Value			
Nozzle Temperature (°C)	190	200	210*	220
Bed Temperature (°C)	25*	50	75	
Layer Thickness (mm)	0.20	0.25*	0.3	
Printing Speed (mm/min)	150	300*	450	

\*These values were kept constant while investigating other parameters.

CFRTP printing usually requires a filament cutter at the end of the layers and discontinuities. In this study, a custom G-code was written to eliminate the cutting of the fibers during printing. The printing path of the CFRTP samples is given in Figure 1. As seen from the figure, an elliptical-shaped printing path was chosen. Excessive parts at both ends were cut at the end of the printing process. Two remaining rectangular shapes are three-point bending test samples. Distance between two samples is carefully chosen to avoid printing sharp corners, which tend to cause failure in CFRTP printing.

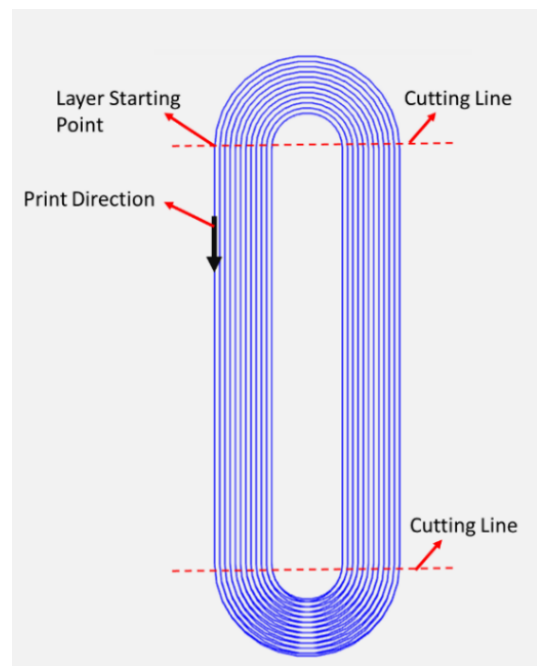


**Figure 1.** Printing path of the CFRTP samples

### 2.3 Three-point bending tests

Three-point bending samples were manufactured following the ISO 14125 standard [26]. Samples have dimensions of 100×15×2 mm<sup>3</sup>. MTS Criterion Model 45 testing machine was used with 10 kN load capacity to perform three-point bending tests. Crosshead velocity was selected as 5 mm/min in accordance with the standards. Supports were positioned at an 80 mm distance. A 5 mm indenter with a circular cross-section was used. At least four tests were carried out for each parameter to verify the results. Images of the three-point bending tests and printed parts are shown in Figure 2.

After the tests, force and deflection data were taken from the test platform. Formula 1-3 were used to calculate flexural strength, strain, and elasticity of modulus where  $\sigma_f$  is flexural

strength,  $\epsilon_f$  is flexural strain,  $E$  is the flexural elasticity of the sample,  $F$  is the load,  $L$  is the distance between the supports,  $D$  is the deflection of the center,  $b$  is the width of the specimen,  $d$  is the thickness of the specimen and  $m$  is the slope of the force load curve from the elastic region.

$$\sigma_f = \frac{3FL}{2bd^2} \quad (1)$$

$$\epsilon_f = \frac{L^2}{6Dd} \quad (2)$$

$$E = \frac{mL^3}{4bd^3} \quad (3)$$

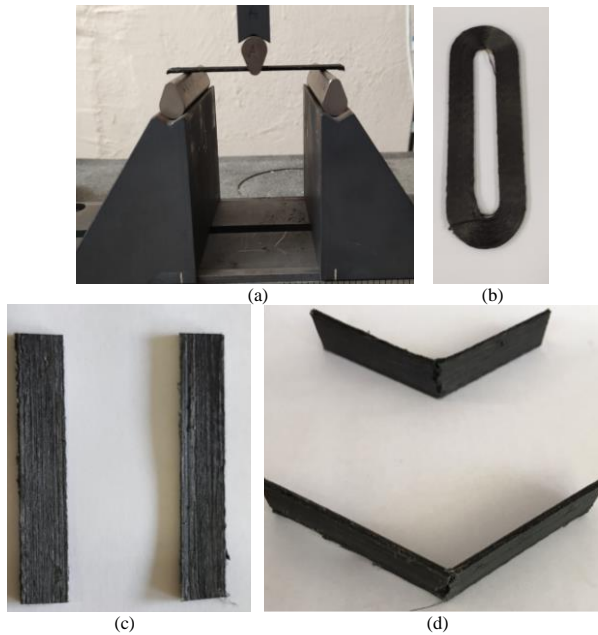


**Figure 2.** Application of three-point bending tests; a) testing platform, b) three-point bending test sample before cutting, c) test samples after cutting, and d) test sample after the test

### 3. Results and discussion

Firstly, CFRTP samples were printed using different nozzle temperatures ranging from 190-220°C. Obtained stress-strain diagrams are shown in Figure 3. The figure shows that the 220°C samples have the highest flexural properties compared to other samples. Lower nozzle temperature samples (200°C and 190°C) have similar results, but the 200°C samples have slightly higher flexural properties. Usually, PLA used in this study has a suggested printing temperature between 190-210°C, but continuous fiber tends to conduct and disperse the heat, requiring higher than recommended nozzle temperatures to print [27]. Results obtained from these tests are summarized in Table 2. From the table, it can be said that 220°C samples have shown the highest flexural strength (172 MPa) and flexural modulus (14 GPa). When the studies in the literature are examined, it can be stated that increasing printing temperature and increasing flexural strength can be achieved [28,29]. A similar effect was observed in this study using CFRTP filaments. An increased rate of flexural strength and modulus according to the printing temperature was added to Table 2. Usually, printing with neat PLA, an increase in mechanical properties can be very small with the increasing printing temperature [30,31] depending on various other conditions. But with continuous additives, a significant increase in mechanical properties can be observed

with the increasing printing temperature [27,32]. From Table 2, it can also be stated that an increase in flexural modulus can be observed with the increasing temperatures.

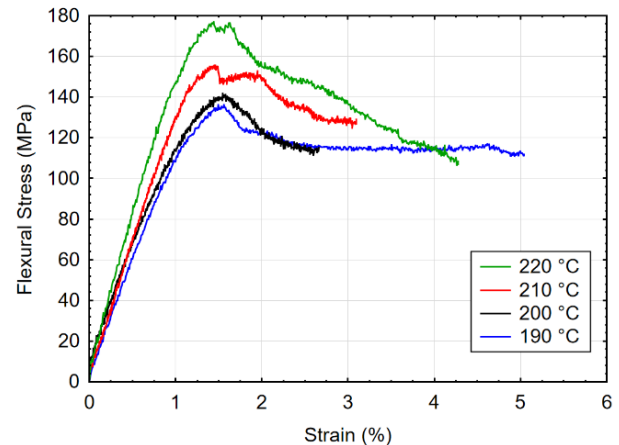


**Figure 3.** Effect of nozzle temperature on three-point bending stress-strain diagrams

Similarly, heated bed temperatures were investigated, ranging between room temperature (around 25°C) to 75°C. Stress-strain diagrams obtained from different bed temperatures are shown in Figure 4. As seen from the figure, the 75°C samples have shown significantly higher flexural properties. On the other hand, the 50 °C samples have shown very similar results to the sample printed at room temperature. Therefore, it can be said that this temperature value had little to no effect on flexural strength. On the other hand, it can be seen that the 50 °C test sample has shown almost twice the failure strain value, which indicates that higher bed temperatures prevent premature failure due to weak interlayer bonding.

**Table 2.** Summary of three-point bending test results with different nozzle temperatures (standard deviations were given in the brackets)

Nozzle Temperature (°C)	Flexural strength (MPa)	Increase in flexural strength (%)	Flexural Modulus (GPa)	Increase in flexural modulus (%)
190	141.80 (14.3)	-	12.78 (1.71)	-
200	143.09 (21.9)	0.91*	12.53 (2.28)	-1.96*
210	157.39 (14.7)	10.99*	13.65 (0.89)	6.81*
220	172.32 (7.6)	21.52*	14.03 (1.68)	9.78*

\*These values are calculated with comparison to 190°C nozzle temperature samples.

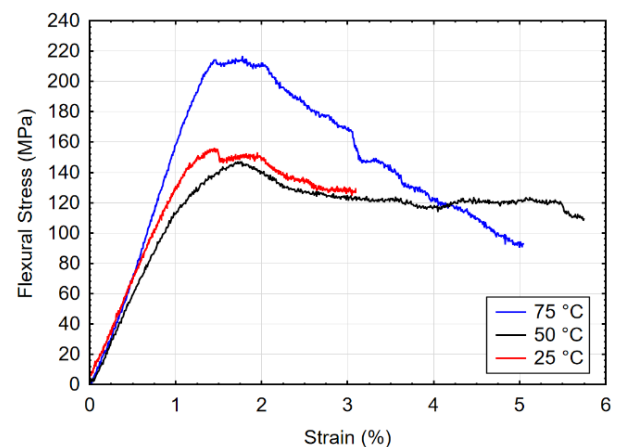


**Figure 4.** Effect of heated bed temperature on three-point bending stress-strain diagrams

Results obtained from these different heated bed parameter tests are summarized in Table 3. From the table, it can be said that 75°C samples have shown the highest flexural strength of 224 MPa and flexural modulus of 14.7 GPa. Chadha et al. [33] observed an increase in the flexural strength with the increasing bed temperature up to 60°C with printing neat PLA. In this study, the effects of the bed temperature on flexural strength are significantly increased after 50°C due to the fiber content. Also, it can be said that increasing bed temperatures up to 50°C showed a decrease in the flexural modulus, but 75°C samples showed the highest.

**Table 3.** Summary of three-point bending test results with different heated bed temperatures (standard deviations were given in the brackets)

Heated Bed Temperature (°C)	Flexural strength (MPa)	Increase in flexural strength (%)	Flexural Modulus (GPa)	Increase in flexural modulus (%)
25	157.39 (14.7)	-	12.78 (1.71)	-
50	154.3 (15.3)	-1.96*	12.89 (2.16)	0.86*
75	223.7 (12.1)	42.13*	14.70 (0.56)	15.02*

\*These values are calculated with comparison to 25°C heated bed samples.

Stress-strain diagrams obtained from different layer thicknesses are shown in Figure 5. Results obtained from these different layer thickness tests are summarized in Table 4. As seen from the figure, these samples have shown very similar mechanical properties. But standard deviation of 0.2 mm and 0.3 mm layer thickness test samples are significantly higher. In lower layer thickness values, the nozzle damages the fibers and decreases the mechanical properties and print quality. On the other hand, higher layer thickness values have fewer layers which affect the part to have slightly higher mechanical properties. Additionally, it can be said that an increased flexural modulus was achieved with the increasing layer thickness.

**Table 4.** Summary of three-point bending test results with a different layer thickness (standard deviations were given in the brackets)

Layer Thickness (mm)	Flexural strength (MPa)	Increase in flexural strength (%)	Flexural Modulus (GPa)	Increase in flexural modulus (%)
0.2	158.48 (26.73)	-	12.65 (2.18)	-
0.25	157.39 (14.7)	-0.69*	12.78 (1.71)	1.03*
0.3	158.22 (44.61)	-0.16*	13.25 (3.34)	4.74*

\*These values are calculated with comparison to 0.2 layer thickness samples.

Stress-strain diagrams obtained from different printing speeds are given in Figure 6. As seen from the figure, a significant drop in the flexural strength and flexural modulus can be observed as the printing speed increases as expected [27,34]. This effect is mainly caused by the damages in CFRTP filaments at faster printing speeds. Additionally, in slower printing, the nozzle preheats the incoming printing area, causing stronger interlayer bonding. Results obtained from different printing speeds are summarized in Table 5. Furthermore, 450 mm/min samples have shown much more ductile behavior compared to other printing speed samples despite having the lowest flexural strength. This is observed because the applied forces on testing are not transferred to the fibers efficiently, which shows similar mechanical behavior to the neat PLA.

**Table 5.** Summary of three-point bending test results with different printing speeds (standard deviations were given in the brackets)

Printing Speed (mm/min)	Flexural strength (MPa)	Increase in flexural strength (%)	Flexural Modulus (GPa)	Increase in flexural modulus (%)
450	107.53 (17.83)	-	9.67 (1.86)	-
300	157.39 (14.7)	46.37*	12.78 (1.71)	32.16*
150	210.76 (26.21)	96.00*	17.69 (2.11)	82.94*

\*These values are calculated with comparison to 450 mm/min printing speed samples.

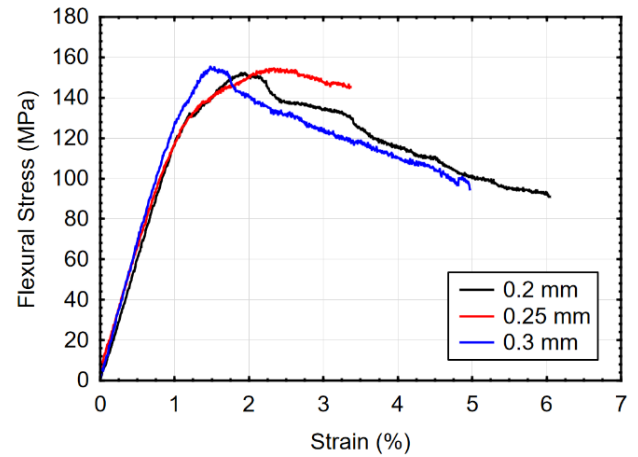


**Figure 5.** Effect of layer thickness on three-point bending stress-strain diagrams

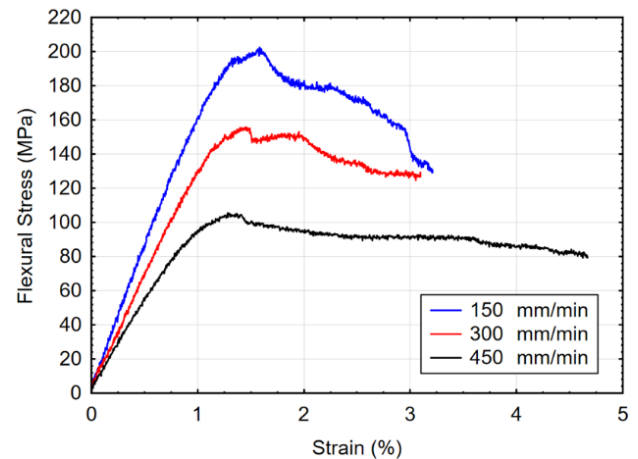


**Figure 6.** Effect of printing speed on three-point bending stress-strain diagrams

#### 4. Conclusions

In this study, CFRTP pre-preg filaments were manufactured using the melt impregnation method. In addition, FDM based additive manufactured method was utilized to obtain test samples. Effects of printing parameters of CFRTP samples were investigated using flexural testing. Investigated parameters can be listed as nozzle temperature, heated bed temperature, printing speed, and layer thickness. Flexural testing showed that heated bed temperature and printing speed significantly affect mechanical properties. Slower printing speed and higher temperatures both with nozzle and the heated bed showed an increase in overall flexural properties of the printed CFRTP samples. In this study, the highest achieved flexural strength is 224 MPa, and flexural modulus is 18 GPa with a 23% fiber ratio.

## Acknowledgments

This work was supported by The Scientific and Technical Research Council of Turkey (TÜBİTAK) with grant number 120M717 and the Office of Scientific Research Projects of Karadeniz Technical University, Turkey, with the grant number FBA-2020-8974.

## Author contributions

Altuğ Uşun: Writing - Original Draft, Methodology, Investigation, Data Curation, Visualization, Writing, Review & Editing.

Recep Gümrük: Literature Search, Conceptualization, Supervision, Funding acquisition, Methodology.

Nuri Yıldız: Data Curation, Visualization, Writing, Review & Editing.

Bahri Barış Vatandaş: Investigation, Data Curation, Writing, Review & Editing.

## References

1. Yu, H., Hong, H., Cao, S. & Ahmad, R. Topology optimization for multipatch fused deposition modeling 3D printing, *Appl. Sci.*, **2020**, 10
2. Rezaie, R., Badrossamay, M., Ghaei, A. & Moosavi, H. Topology optimization for fused deposition modeling process, *Procedia CIRP*, **2013**, 6, 521–526
3. Karamooz Ravari, M. R., Kadkhodaei, M., Badrossamay, M. & Rezaei, R. Numerical investigation on mechanical properties of cellular lattice structures fabricated by fused deposition modeling. *Int. J. Mech. Sci.*, **2014**, 88, 154–161
4. Gümrük, R. & Mines, R.A.W., Compressive behaviour of stainless steel micro-lattice structures, *Int. J. Mech. Sci.*, **2013**, 68, 125–139
5. Behera, M.P., Dougherty, T., Singamneni, S., Conventional and additive manufacturing with metal matrix composites: A perspective, *Procedia Manuf.*, **2019**, 30, 159–166
6. Pereira, T., Kennedy, J.V., Potgieter, J., A comparison of traditional manufacturing vs additive manufacturing, the best method for the job, *Procedia Manuf.*, **2019**, 30, 11–18
7. Gao, A., et al., Highly conductive and light-weight acrylonitrile-butadiene-styrene copolymer/reduced graphene nanocomposites with segregated conductive structure, *Compos. Part A Appl. Sci. Manuf.*, **2019**, 122, 1–7
8. Matsuzaki, R., et al., Three-dimensional printing of continuous-fiber composites by in-nozzle impregnation, *Sci. Rep.*, **2016**, 6, 1–7
9. Liu, G., Xiong, Y., & Zhou, L., Additive manufacturing of continuous fiber reinforced polymer composites: Design opportunities and novel applications, *Compos. Commun.*, **2021**, 27, 100907
10. How Wartsilä Created the First CE-Certified Lifting Tool, <http://static.markforged.com/downloads/WartsilaCaseStudy.pdf>, Last accessed: 13.07.2022
11. Haddington Dynamics: 7-Axis Robotic Arm, <https://markforged.com/additive-manufacturing-movement/haddington-dynamics-7-axis-robotic-arm>, Last accessed: 13.07.2022
12. Penumakala, P.K., Santo, J., & Thomas, A., A critical review on the fused deposition modeling of thermoplastic polymer composites, *Compos. Part B Eng*, **2020**, 201, 108336
13. Krajangsawasdi, N., et al., Fused Deposition Modelling of Fibre Reinforced Polymer Composites: A Parametric Review, *J. Compos.*, **2021**, 5, 29
14. Matsuzaki, R., et al., Three-dimensional printing of continuous-fiber composites by in-nozzle impregnation, *Sci. Rep.*, **2016**, 6, 1–7
15. Li, H., Wang, T., Joshi, S., & Yu, Z., The quantitative analysis of tensile strength of additively manufactured continuous carbon fiber reinforced polylactic acid PLA, *Rapid Prototyp. J.*, **2019**, 25, 1624–1636
16. Araya-Calvo, M., et al., Evaluation of compressive and flexural properties of continuous fiber fabrication additive manufacturing technology, *Addit. Manuf.*, **2018**, 22, 157–164
17. Chacón, J. M., et al., Additive manufacturing of continuous fibre reinforced thermoplastic composites using fused deposition modelling: Effect of process parameters on mechanical properties, *Compos. Sci. Technol.*, **2019**, 181, 107688
18. Chen, K., Yu, L., Cui, Y., Jia, M., & Pan, K., Optimization of printing parameters of 3D-printed continuous glass fiber reinforced polylactic acid composites, *Thin-Walled Struct.*, **2021**, 164, 107717
19. Zhang, H., et al., Recent progress of 3D printed continuous fiber reinforced polymer composites based on fused deposition modeling: a review, *J. Mater. Sci.*, **2021**, 56, 12999–13022
20. Liu, T., Tian, X., Zhang, Y., Cao, Y., & Li, D., High-pressure interfacial impregnation by micro-screw in-situ extrusion for 3D printed continuous carbon fiber reinforced nylon composites, *Compos. Part A Appl. Sci. Manuf.*, **2020**, 130, 105770
21. Zhang, J., et al., Performance of 3D-printed continuous-carbon-fiber-reinforced plastics with pressure, *Materials Basel*, **2020**, 13
22. Wang, K., et al., Heat-treatment effects on dimensional stability and mechanical properties of 3D printed continuous carbon fiber-reinforced composites, *Compos. Part A Appl. Sci. Manuf.*, **2021**, 147, 106460
23. Wang, P., & Zou, B., Improvement of Heat Treatment Process on Mechanical Properties of FDM 3D-Printed Short- and Continuous-Fiber-Reinforced PEEK Composites, *Coatings* **2022**, 12, 827
24. Nassar, A., Younis, M., Elzareef, M., & Nassar, E., Effects of heat-treatment on tensile behavior and dimension stability of 3D printed carbon fiber reinforced composites, *Polymers Basel*, **2021**, 13, 1–21
25. Uşun, A., & Gümrük, R., The mechanical performance of the 3D printed composites produced with continuous carbon fiber reinforced filaments obtained via melt impregnation, *Addit. Manuf.*, **2021**, 46
26. European standards, EN ISO 14125, Fibre-reinforced plastic composites, Determination of flexural properties. <https://intweb.tse.org.tr/>, **2011**
27. Tian, X., Liu, T., Yang, C., Wang, Q., & Li, D., Interface and performance of 3D printed continuous carbon fiber reinforced PLA composites, *Compos. Part A Appl. Sci. Manuf.*, **2016**, 88, 198–205
28. Xu, J., Xu, F., & Gao, G., The Effect of 3D Printing Process Parameters on the Mechanical Properties of PLA Parts, *J. Phys. Conf. Ser.*, **2021**, 2133

29. Hsueh, M.H., et al., Effect of printing parameters on the thermal and mechanical properties of 3d-printed pla and petg, using fused deposition modeling, *Polymers Basel.*, **2021**, 13
30. Bazin, M.M., Othman, M.Z.M., Padzi, M.M., & Ghazali, F.A., Optimisation of 3D printing parameter for improving mechanical strength of ABS printed parts, *Int. J. Mech. Eng. Technol.*, **2019**, 10, 255–260
31. Hsueh, M.H., et al., Effects of printing temperature and filling percentage on the mechanical behavior of fused deposition molding technology components for 3d printing, *Polymers Basel*, **2021**, 13
32. Chen, K., Yu, L., Cui, Y., Jia, M., & Pan, K., Optimization of printing parameters of 3D-printed continuous glass fiber reinforced polylactic acid composites, *Thin-Walled Struct.*, **2021**, 164, 107717
33. Chadha, A., et al., Effect of fused deposition modelling process parameters on mechanical properties of 3D printed parts. *World J. Eng.*, **2019**, 16, 550–559
34. Dou, H., et al., Effect of process parameters on tensile mechanical properties of 3D printing continuous carbon fiber-reinforced PLA composites, *Materials Basel.*, **2020**, 13